Spontaneous Formation of Silver Nanoparticles in Multilamellar Vesicles

Chrystel Faure,* Alain Derré, and Wilfrid Neri

Centre de Recherche Paul Pascal (CNRS), Avenue du Dr. Albert Schweitzer, 33600 Pessac, France

Received: November 13, 2002; In Final Form: February 25, 2003

Silver nanoparticles have been synthesized using $AgNO_3$ as the metallic source and onion-type multilamellar vesicles (MLV) as the microreactor, where the Genamin T020 organic component is acting as the reductant. Silver ions were introduced into MLV either by diffusion from the dispersion medium, or directly by mixing $AgNO_3$ solution with Genamin T020 followed by a shear process. Both the effect of synthetic routes and aging upon the nanoparticle size and assemblies are studied by TEM. In the former case, the size of silver nanoparticles increases from ca. 3 nm to 9.6 nm with increasing dispersion time (30 min and 17 h respectively). For short dispersion times, silver nanoparticles assemble in circular aggregates. The typical size of those aggregates resembles that of MLV, thus indicating an in-situ synthesis. In the latter case, nanoparticle growth is quicker: 7−8 nm silver particles being synthesized in 30 min. Nanoparticles arrange themselves then in parallel strings separated from each other, forming planes, stacked on each other in some cases. A higher onion internal pH measured by ^{31}P NMR is assumed to induce Ag_2O precipitation inside onions contributing to Ag(I) reduction in metallic nanoparticles.

Introduction

Nanoparticle synthesis has attracted much attention in the recent years[1] as a result of their optical, electronic, magnetic, and chemical properties and their subsequent technological potential applications. Silver colloids are mainly used in photographic reactions,[2] catalysis,[3,4] and chemical analysis.[5] Less known is their biological interest, notably because of their ability to inactivate bacteria and some viruses,[6] hence their use for antimicrobial purposes for instance.

Many strategies have been employed for silver nanoparticle synthesis in aqueous media: chemical reduction in the presence of a stabilizing agent,[7−9] electrochemistry,[10] sol−gel processes,[11] RESOLV method,[12] etc. Generally, when silver particles in the nanometer-scale or patterned arrays of silver nanoparticles are wanted, one resorts to assembled organic templates: dendrimers,[13] lyotropic liquid crystals,[14] reverse microemulsions.[15,16] However, in all the quoted examples, reduction is either chemically[14,16] or photochemically induced.[13,15] Qi et al.[17] show that silver nanoparticles can be synthesized within lamellar lyotropic liquid crystals without any external chemical reductant or photochemical treatment making use of the surfactant itself as a reductant. However, they report that synthesis at room temperature requires a much longer aging time (several days) than at 50 °C. Esumi et al.[18] also succeeded in preparing silver nanoparticles into sugar-ball dendrimers without requiring chemical or photochemical treatment. They assumed that dendrimers were responsible for the "spontaneous" Ag(I) reduction. It is worthwhile to note that synthesis occurred only in the presence of NaOH.

In this paper, we report a real "spontaneous" and rapid formation of silver nanoparticles in onion-type multilamellar vesicles. Two preparative strategies are compared: the "one-step" synthesis by manually shearing the lamellae-forming surfactant GT020 with $AgNO_3$ and subsequent dilution of the obtained MLV in water, and the "two-step" synthesis where MLV were first prepared from manually shearing GT020 with water and were then dispersed in $AgNO_3$ solution. Both strategies lead to the synthesis of nanometer-sized silver nanoparticles, but significant differences are shown in particle assembling and kinetics of nanoparticle growth. Genamin T020 is assumed to play a triple role in silver particle formation: (i) as a base, it increases the internal pH of MLV as evidenced by ^{31}P nuclear magnetic resonance, inducing in-situ Ag_2O precipitation; (ii) as a reductant; and (iii) as a surfactant it stabilizes the formed silver particles.

Materials and Method

Materials. Silver nitrate ($AgNO_3$, 99+%) was purchased from Aldrich. Genamin T020 (GT020) is a nonionic surfactant, a mixture of fatty ethoxylated amines whose formula is $R-N[(C_2H_4O)_xH][(C_2H_4O)_yH]$ where $x + y = 2$. Most of the aliphatic chains contain 18 atoms of carbon. It was provided by Clariant GmbH. All reagents were used without further purification. Water was purified with a Barnsted E-pure water purifier.

Preparation of Multilamellar Vesicles Containing Silver Nanoparticles. Onion-type multilamellar vesicle formation has been largely detailed in the literature[19−21] so that we will provide only the main features for a better understanding of our study. It has been shown that, under shearing, a lamellar phase can rearrange into a phase of multilamellar vesicles—so-called onions—compactly packed in space. For some lamellar compositions and notably for ours, a crude, manual shearing is sufficient to get multilamellar vesicles. If an "active" molecule, such as a metallic salt, is solubilized in the aqueous part of the lamellar phase, shearing will result in this molecule encapsulation into the multilamellar vesicles. Onions in close contact can then be dispersed in an excess of water to give a colloidal dispersion. The encapsulated molecules will remain inside the onions providing a large size (like an enzyme[22,23] or DNA[24]), or an affinity for the membrane.[21]

* Corresponding Author. Phone: (33)556845665. Fax: (33)556845600. E-mail: faure@crpp.u-bordeaux.fr.

10.1021/jp027449u CCC: $25.00
Published on Web 04/26/2003

Multilamellar vesicles containing silver nanoparticles were prepared using two different methods:

1. Multilamellar vesicles were first prepared by shearing 0.5 g of GT020 with 0.5 g of water with a spatula until a homogeneous paste was obtained.[25] An amount of 100 mg of the paste was then dispersed in 1 mL of water by mechanical rotation using a vortex stirrer (600 rpm). Once the multilamellar vesicles were dispersed in water, 1 mL of 0.44 M $AgNO_3$ solution was added to the aqueous dispersion. The dispersion was then allowed to "incubate" at room temperature. For these samples, the silver salt diffuses through the lamellae of the vesicles, and silver particles are formed in the vesicles. Let us note that, for these samples, what we define as the "incubation time" in the following part of the document is actually the dispersion time.

2. Multilamellar vesicles were prepared by shearing with a spatula 0.5 g of GT020 with 0.5 g of 0.44 M $AgNO_3$ solution until a homogeneous paste was obtained, which takes 5−10 min. The paste was allowed to incubate at room temperature, and dispersion of MLV in water is thereafter performed for TEM analysis. In that case, the silver salt is used both to hydrate the surfactant and to form the lamellar phase. This salt is thus "encapsulated" in the multilamellar vesicles where reduction into silver nanoparticles occurs. Let us note that, for these samples, the "incubation time" is the period that precedes the MLV dispersion in water.

^{31}P Nuclear Magnetic Resonance. ^{31}P NMR experiments were performed at 121 MHz using a Bruker ARX300 spectrometer at 300 ± 1 K.

The T_1 for inorganic phosphate was determined to be 1.7 s with $\pi/2 = 12.25$ μs. The pulse width was set to 4 μs with a recycle time of 0 s. The dwell time was 300 μs, with 2K real data points. Spectra consist of 2000 acquisitions. Chemical shifts are reported relative to an external reference: phosphoric acid placed in a capillary inserted inside the 10 mm NMR tube, with shifts downfield were reported as positive.

Transmission Electron Microscopy and Size Distribution. TEM measurements were performed on a JEOL 2000FX, working under an acceleration voltage of 200 kV and equipped with an EDXA detector.

For the analysis, a drop of the multilamellar vesicle suspension was deposited onto a carbon film supported by a copper grid and the solvent was allowed to evaporate. For samples prepared by direct hydration of the surfactants with $AgNO_3$, multilamellar vesicles were dispersed in water (3.5 mg of paste/1 mL of water) just before the preparation of the grids. The size distribution of the silver nanoparticles was derived from the measurement of digitized micrographs. The mean diameter, d, and the standard deviation, σ, are obtained from an average of 100 particles. The polydispersity is defined as σ/d.

X-ray Diffraction. X-ray diffraction was carried out with an INEL CPS120 X-ray diffractometer, using filtered Cu Kα radiation. The patterns were recorded in the 2θ range 10−100°. The temperature of the collection data is 25 °C. Samples were centrifuged at 3000 rpm for 10 min. The sediment was deposited on a glass slide covered by a thin layer of grease and allowed to evaporate for 2 h.

Results and Discussion

As already mentioned above, two different strategies can be used to synthesize silver nanoparticles in the multilamellar vesicles: either onions composed of GT020−water were first prepared and then immediately dispersed in an $AgNO_3$ solution, or $AgNO_3$ solution was "encapsulated" inside onions and, later on, onions were dispersed in water. In the following, we will consider both methods of synthesis separately.

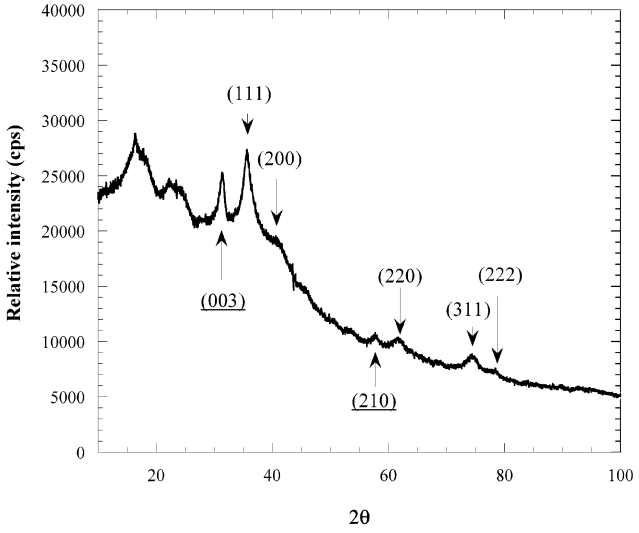

Figure 1. Diffraction pattern of precipitates obtained from centrifuging a 48-h-aged suspension of multilamellar vesicles in $AgNO_3$ solution. Peaks are indexed. Underlined numbers correspond to Ag_2O planes, and crude numbers refer to Ag planes.

Synthesis of Silver Nanoparticles When Silver Ions Are Introduced in the Dispersion Medium. Before addition of $AgNO_3$ solution, the dispersion of onions in water is slightly yellowish. Upon addition of the silver salt solution, the onion suspension gradually changes to a pink/light-brown color after 30 min, then gradually turns to a darker-brown color with time. Multilamellar vesicles slowly sediment: a small dark-brown, turbid sediment is formed after 2 h, and complete sedimentation requires ca. 2 days. The pellet consists of onion aggregates as observed by phase contrast microscopy, whereas the supernatant, a very light-brown limpid solution, is almost devoid of vesicles. The onion aggregates break out through manual agitation and MLV can then be redispersed.

To identify the sediment components, X-ray diffraction analysis was carried out on a centrifuged dispersion, which was aged for 48 h. The XRD pattern of the dried sediment is shown in Figure 1. Five peaks correspond to silver with cubic symmetry:[26] the corresponding atomic layer spacings are 2.33, 2.07, 1.43, 1.22, and 1.17 Å which correspond to {111}, {200}, {220}, {311}, and {222} crystallographic planes, respectively. These values are in good agreement with the reported data (JCPDS, n°4-0783). Two broad peaks are also observed at the lowest 2θ angle values, which can be assigned to the SiO_2 support and the grease that were used to prepare samples. Convoluted to those broad peaks, four narrow peaks can be detected but they could not be assigned with certainty. One can assume three of them (ca. 19°, 22°, and 25°) come from orthorhombic $AgNO_3$ crystallites, but the agreement between theoretical (JCPDS, n°6-363) and experimental values is not good enough to unambiguously assign them. Two other reflection peaks are detected at 2.62 and 1.52 Å. These spacings could be attributed to Ag_2O crystals with hexagonal symmetry (corresponding to {003}and {210} lattice planes, respectively, JCPDS, n°42-874) even though such attribution is surprising, taking into account our experimental conditions. Ag_2O indeed usually crystallizes in cubic symmetry, whereas hexagonal symmetry is usually produced under drastic conditions, such as high pressure. Such unusual crystallization maybe resulted from a confinement effect. Let us note that all the peaks are broad, suggesting the presence of small particles.

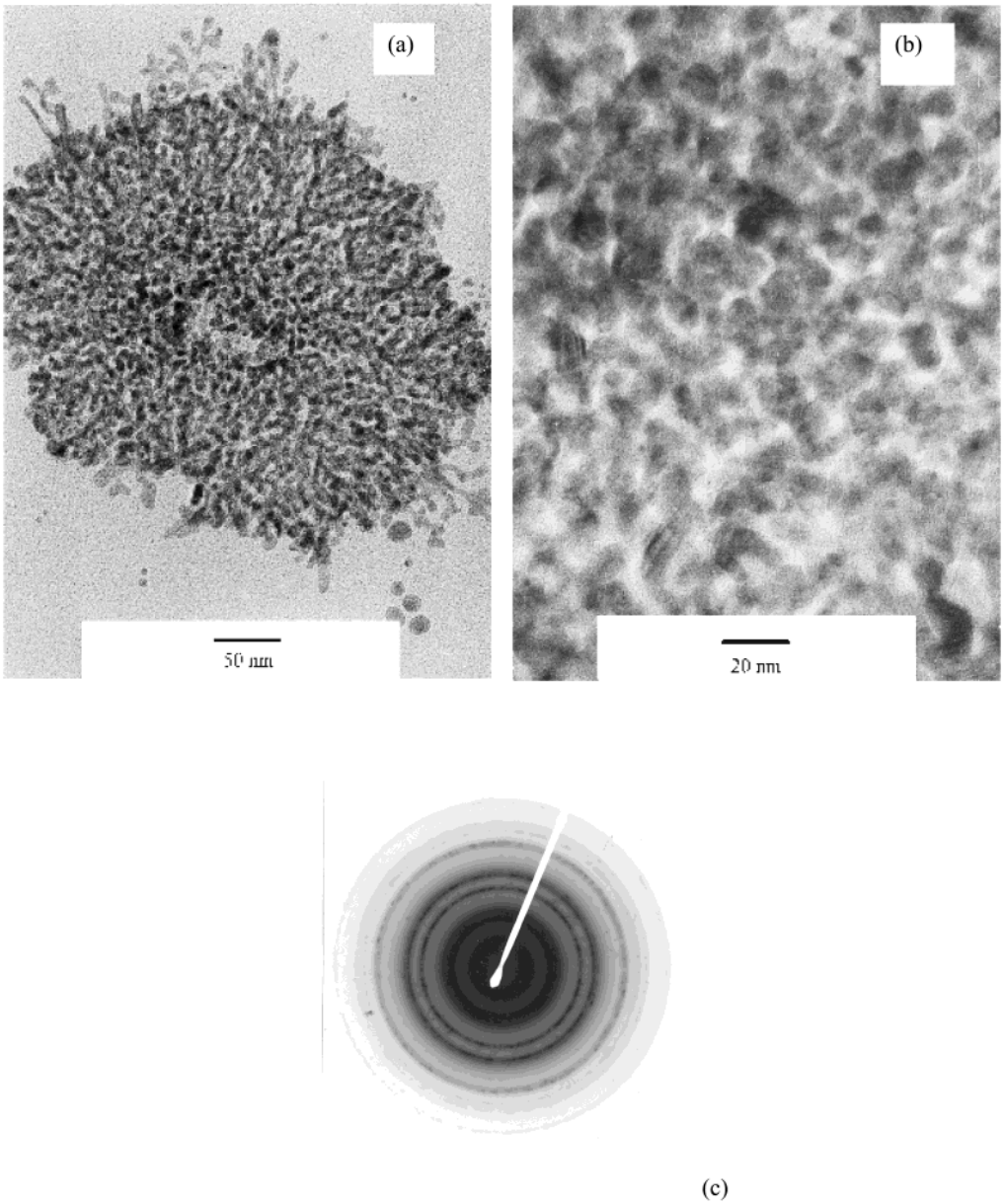

Figure 2. TEM micrographs of a 30-min-aged suspension of multilamellar vesicles in $AgNO_3$ solution, showing (a) circular aggregate of silver nanoparticles, (b) the corresponding expanded picture, and (c) electron diffraction pattern.

Thirty-Minute-Aged Samples. Direct imaging of the as-synthesized particles can be obtained by transmission electron microscopy. Figure 2 displays the corresponding micrographs for onions dispersed in 0.22 M $AgNO_3$ solution for 30 min. TEM observations were run within 1 h after the preparation. Two different structures are visible by TEM: nanoparticles regrouped either in circular large structures or randomly distributed individual nanoparticles (not shown).

One example of the former structure is visible in Figure 2a. The size (ca. 0.3 μm) suits that of the multilamellar vesicles. In the expanded image (Figure 2b), we can observe that these circular aggregates consist of nanoparticles whose size is hardly measurable because of their density; however we can estimate a size smaller than 10 nm. These nanoparticles were analyzed by electron diffraction directly on the microscope. The ED pattern (Figure 2c) shows concentric circles resulting from the random orientation of crystal planes. On the basis of diffraction, a silver face-centered-cubic (fcc) cell with $a = 0.408$ nm cell parameter can be derived, in agreement with XRD observations. Well-separated silver nanoparticles are also present in that kind of sample. Most of the particles are not spherical and are probably coalesced particles formed on the grid (not shown).

TEM observations differ when samples were treated with an excess of a propanol (50 vol %)/cylohexane (50 vol %) solution in order to destroy the multilamellar structures. Circular aggregates (0.3 μm size) are not present anymore, but we can observe single nanoparticles with spherical shape. As seen in Figure 3, most of the nanoparticles have an average estimated size of 3 nm with a very narrow monodispersity. In addition to this main size distribution, a few particles with size ranging from 5 to 30 nm have also been formed.

Seventeen-Hour-Aged Samples. TEM analysis was performed on vesicles dispersed in 0.22 M $AgNO_3$ solution for 17 h instead of for 30 min. In this experiment, no organic solvent was added to destroy onions. Contrary to circular large structures reported in Figure 2a, agglomerates of discrete nanoparticles were observed by TEM (Figure 4a). When focusing (Figure 4b), nanoparticles appear spherical and coalescence is not observed.

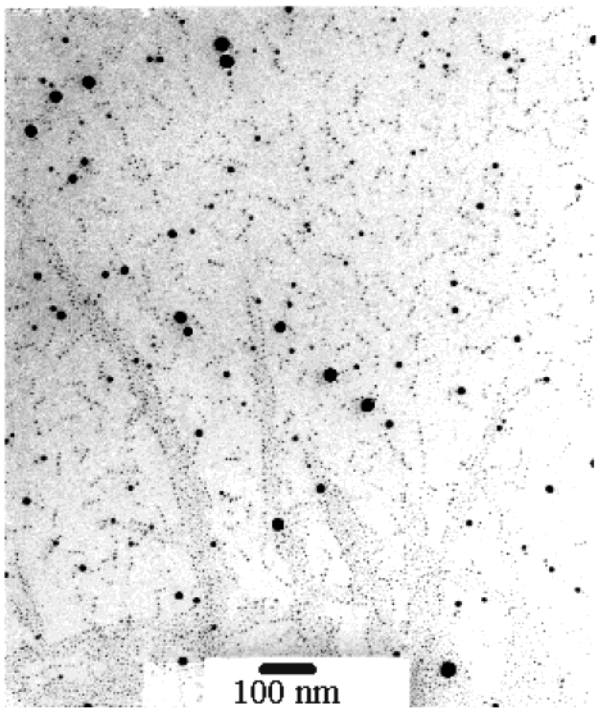

Figure 3. TEM micrograph of silver nanoparticles after dissolving multilamellar vesicles with a propanol (50 vol %)/cyclohexane (50 vol %) solution.

The mean diameter size and polydispersity calculated from the size histogram (Figure 4c) is 9.6 nm and 0.34, respectively. The ED pattern (Figure 4d) proves that these silver nanoparticles are metallic with a face-centered-cubic structure.

Synthesis of Silver Nanoparticles When Silver Salt Is Introduced in the Lamellar Phase. In this section, nanoparticles are grown directly in the lamellar phase in a one-step process. The silver salt is indeed mixed with the surfactant, and the mixture is manually sheared to give a paste which turns brown 15 min after mixing surfactant and metallic salt. The brown color darkens with time. We checked by phase contrast microscopy that this brown paste is composed of MLV once dispersed in water.

Figure 5 shows both types of nanoparticles aggregates observed by TEM on 30-min-aged onions, diluted in water just before TEM grid preparation. As can be seen, anisotropic particle arrangements which look like "batons" (micrograph a) and particle isotropic arrangements (micrograph b) coexist in that sample. The former assemblies are enlarged on Figure 6, which shows that those anisotropic arrangements are made of parallel nanoparticles strings. Figure 5a might indicate that there is a typical length associated with those anisotropic assemblies, with an average value of 0.66 μm. Nanoparticles are spherical-like within isotropic arrangements, whereas some of the particles belonging to the anisotropic arrangements appear elongated (Figure 6a). The latter particles seem to result from coalescence of adjacent particles, which mainly occurs along the longer axis. A mean diameter of 7−8 nm is estimated for the aligned silver particles if coalesced particles are disregarded. From Figure 6b, we can hypothesized that several planes, made of aligned nanoparticles, can stack on each other to form 3D-like assemblies. The two large aggregates observed in Figure 5a are of this type.

Bigger nanoparticles are observed within the isotropic aggregates (Figure 5 b). In addition to a 7−8 nm population, some large nanoparticles (from 25 to 100 nm) appeared, probably resulting from coalescence of smaller nanoparticles.

Discussion

Formation of silver nanoparticles from sheared lamellar phase, without adding any chemical reductant, has been evidenced by TEM and electron diffraction analysis in the section described above. With the following section, we will aim to propose a mechanism that depicts the synthesis of silver nanoparticles and discuss their in-situ characteristic, taking in account ^{31}P NMR data. We will also discuss the effect of the preparative strategy on both silver particle sizes and assembling modes.

Mechanism of Silver Nanoparticle Formation. *Role of Ag_2O in Silver Nanoparticle Formation.* In many reported silver syntheses, Ag_2O was assumed to play a role in the reduction process. Most of the time, a basic medium is indeed required for nanoparticle formation. Silver particles have already been synthesized by spontaneous reduction of silver ions in the presence of hydroxyl groups in basic conditions.[18,27−29] Huang et al.[27] report the formation of Ag colloids by reduction of Ag^+ ions in basic and air-saturated solutions of 2-propanol. They propose that reduction of Ag^+ takes place on Ag_2O particles, which result from the interaction of silver ions with OH^-, whereas oxidation of the 2-propanol occurs on the metal particles. Esumi et al.[18] show that Ag^+ ions can be reduced by addition of NaOH in the presence of dendrimers loading OH groups, whereas no reduction takes place without NaOH. It is assumed that silver oxide is reduced on the surface of dendrimers by electron transfer from the hydroxyl group of glucose residues. Dirske et al.[29] also showed that metal particles can be obtained from Ag_2O treated with concentrated KOH.

In some cases, however, formation of silver nanoparticles is performed without any basic surrounding;[17,30] however, the yield of synthesis is very low (around 1%)[30] and the kinetics at room temperature is slow.[17,30]

All those reported results suggest that silver oxide is likely to contribute to metallic silver formation either on a kinetical or a thermodynamical aspect. In our case, Ag_2O was detected by X-ray diffraction in addition to Ag crystals (Figure 1). We think that Ag_2O precipitation mainly takes place inside the multilamellar vesicles where the pH is higher than in the dispersion medium. This can be evidenced by a ^{31}P nuclear magnetic resonance study as reported in the following section.

Determination of pH inside and outside Onions by ^{31}P NMR Study. ^{31}P NMR has already been proved to be an efficient, non-invasive tool for pH determination inside microspheres.[31] Such measurement is possible because of the inorganic phosphate ^{31}P NMR chemical shift dependence with the pH of the solution.

Figure 7 displays this dependence characteristic for standard phosphate solutions (15 mM NaH_2PO_4/Na_2HPO_4 solution) whose pH was measured using a pH meter (empty circles). The theoretical standard curve calculated from the Henderson−Hasselbalch equation with the parameters given in the figure legend is also shown. From that standard curve, pH can be deduced from the ^{31}P NMR chemical shift of inorganic phosphate solution.

In the specific case where two different pH media are present, two peaks should be observed on the ^{31}P NMR spectrum, providing the exchange rate between both media is slower than the NMR time scale (1 μs).[32] ^{31}P NMR experiments were thus carried out on multilamellar vesicles composed of GT020 (50 wt %) and water (50 wt %) dispersed in 15 mM NaH_2PO_4/Na_2HPO_4 solution. The phosphorus-containing solution diffuses

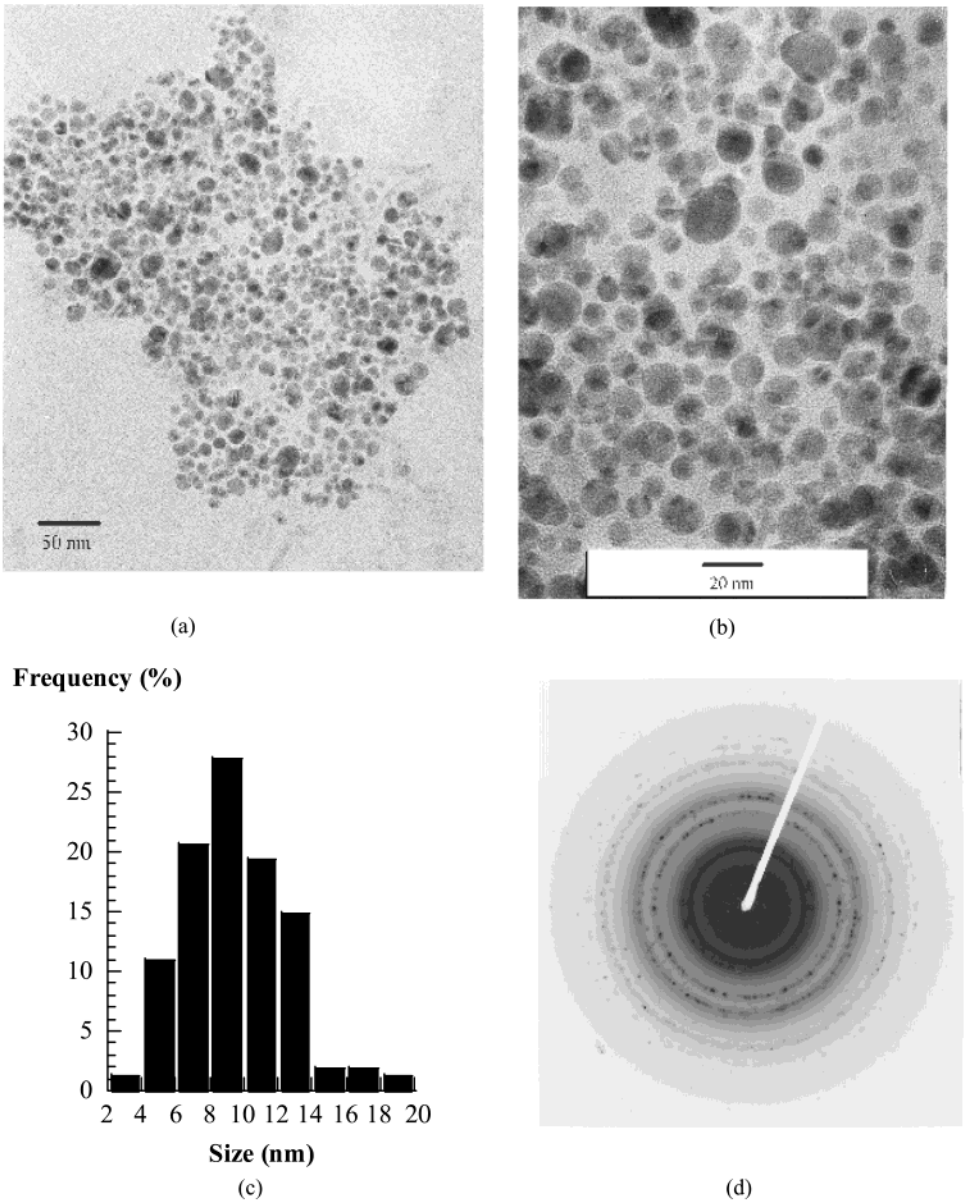

Figure 4. (a) TEM micrograph, (b) expanded photo, (c) size distribution, and (d) electron diffraction pattern of Ag nanoparticles obtained from a 17-h-aged suspension of multilamellar vesicles in $AgNO_3$ solution.

through onion lamellae to achieve osmotic equilibrium. The corresponding ^{31}P NMR spectrum is reported in Figure 8. The intense peak is given by H_3PO_4 solution which serves as an external reference (chemical shift set to 0 ppm). Besides this reference peak, two other peaks are detected. The downfield peak (higher chemical shift) can be assigned to phosphorus atoms present inside the vesicles, whereas the upfield peak (lower chemical shift) can be assigned to phosphorus atoms present in the dispersion solution. This attribution relies on the observed broadening of the downfield peak, which suggests an interaction between phosphorus atoms and the MLV surfactant. On the contrary, when phosphorus atoms are free to move (i.e., when they are in an isotropic medium such as the dispersion solution), the resulting peak is narrow.[32] From the standard curve (Figure 7), we find that pH value is 8.0 and 7.3 inside and outside multilamellar vesicles, respectively. The higher internal pH is caused by GT020, the basic vesicle surfactant (pK_b = 9.1).

The pH difference between the interior and the exterior of the vesicles is not large, 0.7 pH units, but is sufficient to theoretically foresee that silver oxide particles mainly precipitate inside multilamellar vesicles. This conclusion arises from the theoretical curve reported in Figure 9, where the silver ions concentration is plotted as a function of pH. From this curve, the concentration of silver ions, which are in equilibrium with silver oxide when precipitation has occurred, can be deduced. In other words, Figure 9 gives the residual silver ion concentration for a given pH. The graph is shared in two areas: the dashed area contains conditions in which no precipitation takes place, whereas the other area contains conditions in which Ag_2O precipitation from silver ions takes place. From this plot, one can see that for pH > 8.5, most of silver ions precipitate to form Ag_2O and the concentration of residual ions can be read on the *y*-axis, for pH < 6.5, most of silver ions remain in solution, hardly any oxide is formed. Between those two pH values, soluble silver ions and solid silver oxide are in chemical equilibrium; the concentration of the former compound can be deduced from this plot.

Location of Ag_2O Precipitation. When samples are prepared by surfactant hydration with the silver salt aqueous media,

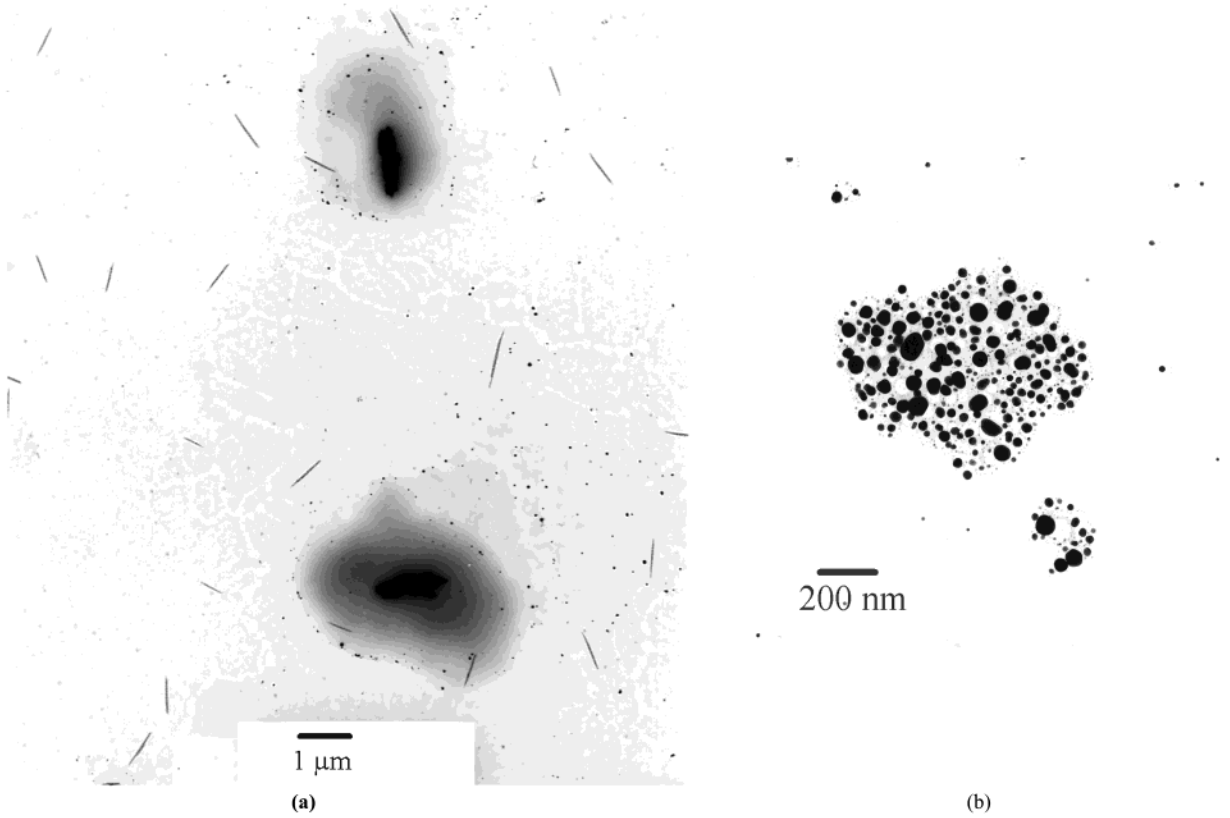

Figure 5. TEM micrographs of a 30-min-aged suspension of multilamellar vesicles hydrated with $AgNO_3$ salt and dispersed in water. (a) Anisotropic arrangements of silver nanoparticles, (b) isotropic aggregates of silver nanoparticles.

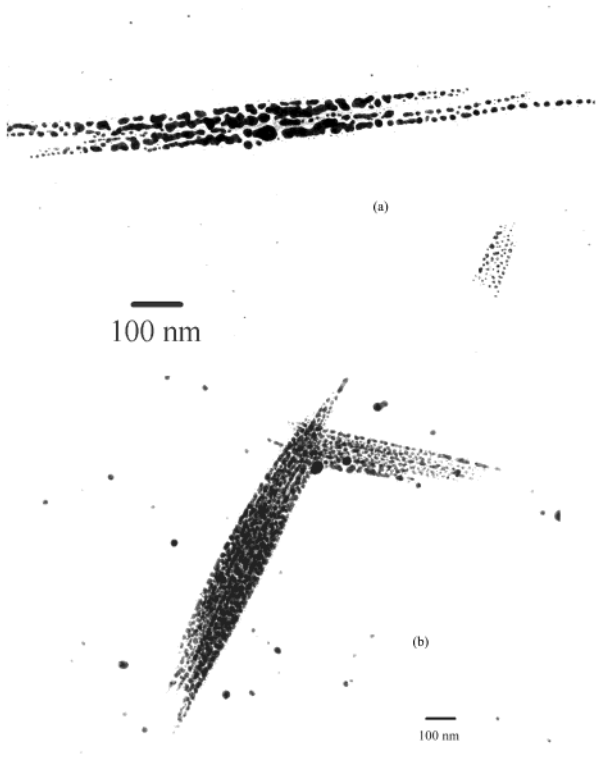

Figure 6. Expanded photos of anisotropic arrangements of silver nanoparticles shown in Figure 5a.

totality of the introduced silver ions (0.22 M) are between GT020 lamellae, and consecutively entrapped inside onions, which are compactly packed after the shearing step. This assessment is based on the phase diagram of a similar system:

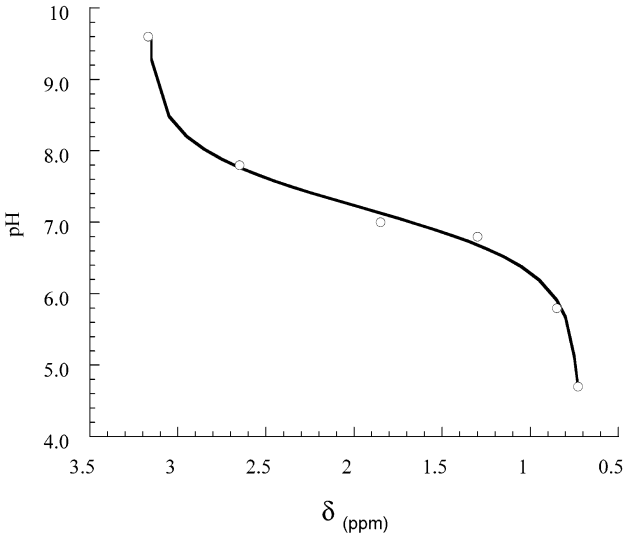

Figure 7. Standard curve for determination of pH by ^{31}P NMR. Experimental points are symbolized by empty circles. Also shown is the theoretical standard curve calculated using the following parameters: $pK_a = 7.2$; $\delta(HPO_4^{2-}) = 3.17$ ppm; $\delta(H_2PO_4^{-}) = 0.73$ ppm.

Genamin T020−$CuSO_4$ solution.[33] For this system, the maximal lamellar phase uptake in salt solution is roughly 70 wt %, so that in our conditions (i.e., a 50 wt % $AgNO_3$ content), it is likely that no excess salt solution coexists with the lamellar phase. This was checked by optical microscopy through polarized light. As pH was measured to be 8.0 inside onions, Figure 9 predicts that precipitation occurs and that soluble silver ions concentration inside onions is ca. 0.02 M (point I, dashed line). This means that roughly all the Ag^+ ions precipitate inside the onions to form silver oxide.

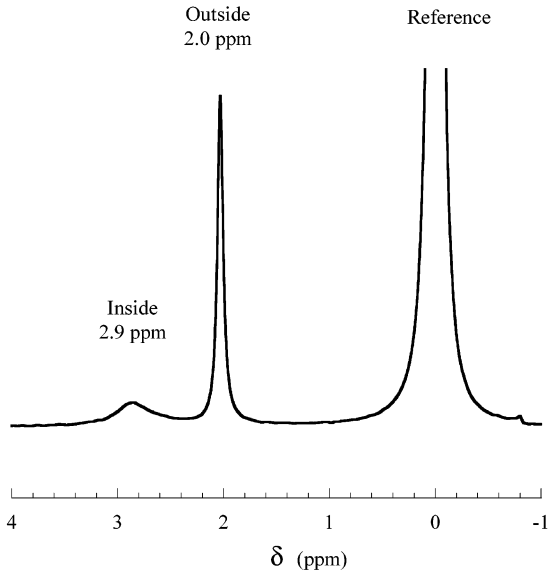

Figure 8. ^{31}P NMR spectrum of GT020 (50 wt %)−water (50 wt %) multilamellar vesicles dispersed in 15 mM NaH_2PO_4/Na_2HPO_4 solution.

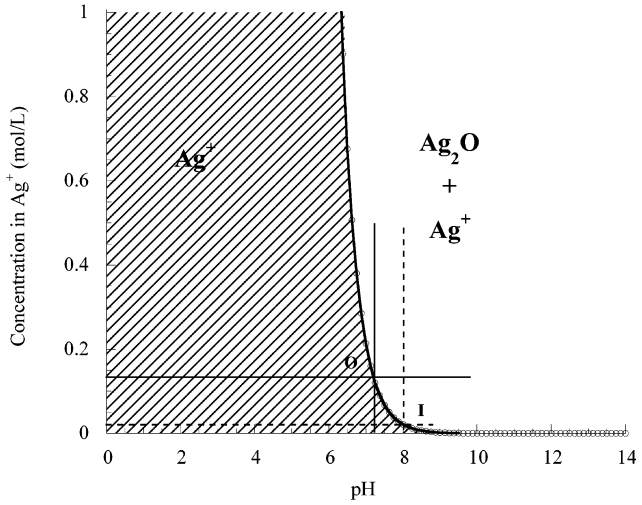

Figure 9. Theoretical curve displaying the concentration of soluble silver ions as a function of pH. The solubility constant value is set to $10^{-15.34}$.[37]

When samples are prepared by diffusion of the salt through GT020 lamellae, a fraction of the silver ions (0.22 M) can precipitate in the dispersion medium, outside onions where pH is 7.3, as concluded from Figure 9: the concentration of soluble silver ions in equilibrium with Ag_2O is theoretically 0.13 M at pH = 7.3 (point O, straight line), which means that roughly half of the silver ions can precipitate outside onions. These ex-situ synthesized Ag_2O particles are perhaps those detected in the X-ray diffraction pattern realized on samples prepared by salt diffusion (Figure 1), even though it is very doubtful that Ag_2O can crystallize in its hexagonal structure outside onions.

In-Situ Character of the Synthesis. The in-situ character of the silver crystallite synthesis is evidenced by TEM micrographs in the case of particles grown by salt diffusion. The confinement of silver particles within circular aggregates shown in Figure 2a,b implies that nanoparticles were synthesized inside multilamellar vesicles. Such TEM observations and conclusions have already been reported in the literature for onions loaded with CuO nanoparticles: copper oxide nanoparticles were produced by chelation of copper ions inside onions and consecutive reduction by hydrazine diffusing through lamellae.[33] Moreover, recent cryo-TEM experiments carried out on onions containing gold nanoparticles clearly evidence that gold nanoparticles are indeed embedded between lamellae.[34] These experiments were performed on samples obtained via the same experimental process, i.e., by surfactant-induced reduction of a metallic salt diffusing through vesicle lamellae. Even though the nature of the nanoparticles differs, these recent results lead us to think that nucleation and growth of nanoparticles mainly occur inside multilamellar vesicles. We can note that an external synthesis of silver nanoparticles cannot be completely ruled out since ^{31}P NMR study indicates that Ag_2O can precipitate outside the onions. Nucleation and growth might then occur on multilamellar vesicles surface. The few 5−30 nm size particles observed in Figure 3 might result from this external synthesis.

When surfactant was directly hydrated with $AgNO_3$ salt, sample composition was chosen in a way where only lamellar phase, without excess salt solution, is formed (see the discussion of the phase diagram in the previous section), which implies that the synthesis occurs within the lamellar phase.

The in-situ character of silver particle formation can be explained both by a higher internal pH as evidenced by ^{31}P NMR and the need of GT020 to reduce Ag(I).

Ag (I) Reduction. As no reducing agent was added in our preparation, the vesicle surfactant Genamin T020 is believed to act as a reductant. This has already been reported for non ionic ethoxylated surfactants.[17,30,35] The conclusion was that surfactants reduce silver ions to the neutral state through oxidation of oxyethylene groups into hydroperoxides,[30] the oxo group was thus essential for the reduction process. Barnickel et al. also achieve the synthesis of colloidal silver particles using ethoxylated surfactant ($C_{12}E_5$-based microemulsions) and conclude that the $C_{12}E_5$ surfactant terminal hydroxyl groups are capable of reducing Ag^+ during UV irradiation.[15] Hydroxyl groups were also assumed to play a role in the reduction process by Esumi et al. who realized Ag(I) reduction with sugar dendrimers.[18] Genamin T020 is a commercial mixture of fatty ethoxylated amines, it bears both oxo and hydroxyl groups, which can thus account for Ag(I) reduction.

Nanoparticle Size and Effect on Onion Structure. When multilamellar vesicles dispersed 30 min in $AgNO_3$ are dissolved by solvent addition, 3 nm size nanoparticles are visualized by transmission electron microscopy. Aging the samples seems to influence both nanoparticle size and vesicle structures. No circular aggregates were indeed detected for a longer dispersion time in the salt medium (17 h), while the average size of metal particles was increased to 9 nm, as the particles polydispersity was increased.

SAXS experiments performed on the GT020−water lamellar phase indicate that membrane thickness is 2.9 nm.[33] For salt-containing lamellae such as GT020−$CuSO_4$ or GT020−$KAuCl_4$, *d* spacing was found to be 5.5 nm[33] and 6.2 nm (obtained by our group), respectively, for a 50 wt % salt solution content. We can thus estimate that aqueous layer thickness is not far from 3 nm. Previous studies on the dependence of the nanoparticle size with water content suggest that once particle size exceeds the water layer thickness, particles are likely to be squeezed out from the lamellar phase.[14,36] This could explain why for 17 h-aged samples, for which nanoparticle size is large (9 nm), no circular aggregates were visible by TEM: particles could have been expelled from onions, inducing their destruction. However, the already mentioned cryo-TEM experiments we carried out on gold-containing onions (see above) have demonstrated that nanoparticles larger than lamellae *d* spacing can remain in the lamellar phase. They obviously generate

defects such as local destructuration and reorganization of the lamellar structure, but not necessarily with complete destruction of the multilamellar template.[34] Lamellae deformation is thus induced by gold particles once their size is greater than the water layer thickness, but no direct evidence of particle expelling and vesicle destruction was brought. For silver nanoparticles, the critical size should be ca. 3 nm, which corresponds to the thickness of an aqueous layer. When silver particle size is smaller than 3 nm, particles probably remain inside onions and the vesicular structure is likely not to be drastically affected. For larger particle sizes, additional experiments are required to give a clear conclusion on the persistence or not of the MLV structure.

When nanoparticles are grown directly in the lamellar phase, i.e., by direct hydration of the surfactant with the silver salt, several differences are noticed. The average size of single nanoparticles is larger, 7−8 nm instead of 3 nm for the same "incubation" time (30 min). Moreover, the samples color change is quicker than observed for onions dispersed in the metallic salt. In that case, silver salt is indeed in direct contact with surfactant, and in such context synthesis is not diffusion-limited; this might explain why larger particles are formed for the same "incubation" time. Moreover, the local salt concentration in the lamellar phase is much higher than for the two-step preparation, which should lead to larger nanoparticles for the same incubation time.

Another difference is that anisotropic particle assemblies are observed. Silver nanoparticles synthesized in lamellar lyotropic liquid crystals have already been shown to arrange in anisotropic assemblies forming ribbons,[17] but their size was larger, i.e., several micrometers long compared to the observed ca. 0.7 μm long. Moreover, the silver nanoparticles were isotropically close-packed and not aligned, also stacks of ribbons were not observed. The preservation of the silver nanoparticle lamellar arrays was attributed to the inherent van der Waals attraction between these particles, whereas delamination of the parallel ribbons was explained by repeated sonications inherent to the TEM sample preparation method.[17]

Surprisingly, in the present work, not only are the nanoparticles aligned within these anisotropic patterns but also the nanoparticles strings are well separated from each other. The latter feature suggests that surfactant in its oxidized state is still present, inserted between particle strings preventing transversal coalescence. For those anisotropic structures, coalescence indeed mainly occurs in the axis of alignment giving elongated silver particles. A possible description of nanoparticle assembling could be that silver particles are confined within cylinders made from bilayers of GT020 in its oxidized state. These cylinders of finite size would be in close contact, forming 2D or 3D patterns. This hypothesis is very speculative, and additional experiments are needed to bring a clear answer.

At first glance, an explanation of the origin of such assembling could be a partial destruction of onions, e.g., once deposited on the grid. This might explain why the size of the anisotropic patterns is limited, since the maximal length expected for onion destructuration is roughly 1 μm—the perimeter of a 0.3 μm size onion—which is in accordance with the 0.66 μm average length measured on Figure 5a. However, the nanoparticle alignment within the anisotropic patterns is hardly understandable, taking into account onion geometry.

Another interpretation could be that they result from a coupling between the shearing process and the fast reduction rate. $AgNO_3$ solution is added to the viscous GT020 liquid, and then both liquids are sheared. The flow induced by spatula mixing combined with the likely fast growth of the nanoparticles might result in alignment of nanoparticles.

Conclusion

The spontaneous synthesis of silver nanoparticles in multilamellar vesicles is reported. The surfactant vesicles was assumed to play a triple role: providing a basic medium for Ag_2O formation, reducing Ag(I) in metal and stabilizing the generated silver nanoparticles. Two protocols for synthesis achievement were compared:(1) direct hydration of the surfactant with the silver ion solution and shearing of the obtained lamellar phase, or (2)diffusion of the silver ions through already formed multilamellar vesicles.

Both methods lead to the synthesis of Ag(0) nanoparticles inside the lamellar phase. The in-situ character of the synthesis is certainly related to the higher internal pH of onions as evidenced by phosphorus NMR, allowing Ag_2O precipitation and the consecutive reduction by vesicle surfactant itself.

For nanoparticles obtained via salt diffusion, the particle size increases with dispersion time of multilamellar vesicles in salt solution, underlining the diffusion-controlled growth of nanoparticles. For short incubation time (30 min), circular aggregates of silver particles were observed by TEM, whereas for longer incubation time (17 h) no such templates were visualized. Vesicle destruction resulting from the increase in particle size could be assumed, but recent cryo-TEM experiments on similar systems indicate that large gold nanoparticles (50 nm) can remain embedded between lamellae without onion destruction.[34]

Nanoparticles synthesized from salt solution directly introduced into the lamellar phase assemble in anisotropic structures, which differ from already-reported silver ribbons[17] obtained from the isotropic lamellar phase, both by their shorter size and the by alignment of the in-plane silver nanoparticles, forming parallel strings separated from each other. These 2D or 3D patterns could result either from a partial destruction of onions on the TEM grid explaining their short size ($<1\mu$m long) compared to those obtained from isotropic spatially distributed lamellar phase,[17] or from a coupling between the shearing process and the fast growth of silver nanoparticles. The nanoparticle alignment as well as the fact that no transversal coalescence occurs suggests that GT020 in its oxidized state is still present in these anisotropic arrays but the nature of its arrangement is very speculative and more studies are necessary to reach a clearest conclusion.

Acknowledgment. We thank Didier Roux, Gilles Sigaud, and Annie Colin for valuable discussion.

References and Notes

(1) Henglein, A. *Chem. Rev.* **1989**, *89*, 1861.
(2) Mostafavi, M.; Marignier, J. L.; Amblard, J.; Belloni, J. *J. Radiat. Phys. Chem.* **1989**, *34*, 605.
(3) Verykios, X. E.; Stein, F. P.; Coughlin, R. W. *Catal. Rev. Sci. Eng.* **1980**, *22*, 197.
(4) Claus, P.; Hofmeister, H. *J. Phys. Chem. B* **1999**, 2766.
(5) Pal, T. *J. Chem. Educ.* **1994**, *71*, 679.
(6) Bateman, P. www.silverinstitute.org 1999.
(7) Henglein, A.; Giersig, M. *J. Phys. Chem. B* **1999**, *103*, 9533.
(8) Wang, W.; Chen, X.; Efrima, S. *J. Phys. Chem. B* **1999**, *103*, 7238.
(9) Jiang, X.; Xie, Y.; Lu, J.; Zhu, L.; He, W.; Qian, Y. *Langmuir* **2001**, *17*, 3795.
(10) Rodriguez-Sanchez, L.; Blanco, M. C.; Lopez-Quintela, M. A. *J. Phys. Chem. B* **2000**, *104*, 9683.
(11) Wu, P. W.; Dunn, B.; Doan, V.; Schwartz, B. J.; Yablonovitch, E.; Yamane, M. *J. Sol−Gel Sci. Technol.* **2000**, *19*, 249.
(12) Ya-Ping, S.; Pornpen, A.; Meziani, M. J. *Langmuir* **2001**, *17*, 5707.
(13) Kéki, S.; Török, J.; Deak, G.; Daroczi, L.; Zsuga, M. *J. Colloid Interface Sci.* **2000**, *229*, 550.

(14) Patkfalvi, R.; Dekany, I. *Colloid Polym. Sci.* **2002**, *280*, 461.
(15) Barnickel, P.; Wokaun, A.; Sager, W.; Eicke, H. F. *J. Colloid Interface Sci.* **1992**, *148*, 80.
(16) Bagwe, R. P.; Khilar, K. C. *Langmuir* **2000**, *16*, 905.
(17) Qi, L.; Gao, Y.; Ma, J. *Colloids Surf., A: Physicochem. Eng. Aspects* **1999**, *157*, 285.
(18) Esumi, K.; Hosoya, T.; Torigoe, K. *Langmuir* **2000**, *16*, 2978.
(19) Diat, O.; Roux, D.; Nallet, F. *J. Phys. II* **1993**, *3*, 1427.
(20) Diat, O.; Roux, D. *J. Phys. II* **1993**, 9.
(21) Gauffre, F.; Roux, D. *Langmuir* **1999**, *15*, 3738.
(22) Olea, D.; Faure, C. *J. Chem. Phys.*, submitted.
(23) Faure, C.; Belamie, E. *Prog. Colloid Polymer Sci.* **2001**, *118*, 42.
(24) Pott, T.; Roux, D. *FEBS Lett.* **2002**, *511*, 150.
(25) Faure, C.; Ravaine, S.; Argoul, F. *J. Electrochem. Soc.* **2000**, *147*, 575.
(26) In *Metal Reference Book, Phys. ed.*; Smithells, C. J., Ed.; Butterworth: Stoneham, MA, 1976.
(27) Huang, Z. Y.; Mills, G.; Hajek, B. *J. Phys. Chem.* **1993**, *97*, 11542.
(28) Dirske, T. P.; Vander Lugt, L. A.; Schnyders, H. *J. Inorg. Nucl. Chem.* **1963**, *25*, 859.
(29) Dirske, T. P.; Vander Hart, D.; Vriesenga, J. *J. Inorg. Nucl. Chem.* **1965**, *27*, 1779.
(30) Liz-Marzan, L. M.; Lado-Tourino, I. *Langmuir* **1996**, *12*, 3585.
(31) Burke, P. A. *Proceed. Intern. Symp. Control. Relat. Bioact. Mater.* **1996**, 133.
(32) Abragam, A. *Principles of Nuclear Magnetism*, 1983 ed.; Oxford University Press: Integrated: London, 1961.
(33) Gauffre, F.; Roux, F. *Langmuir* **1999**, *15*, 3738.
(34) Faure, C.; Regev, O.; Roux, D.; Backov, R. *Adv. Mater.*, submitted.
(35) Barnickel, P.; Wokaun, A. *Mol. Phys.* **1990**, *69*, 1.
(36) Wang, W.; Efrima, S.; Regev, O. *J. Phys. Chem. B* **1999**, *103*, 5613.
(37) Pourbaix, M. In *Atlas d'équilibres électrochimiques*; Cie, G.-V., Ed.; Gauthiers-Villars & Cie: Paris, 1963.